

**Use of Modeling for the Prevention of Solids Formation during Canyon
Processing of Legacy Nuclear Materials**

William J. Crooks III and William D. Rhodes

Strategic Materials Technology Department

Savannah River Technology Center

Jerry D. Christian

Independent Consultant

February 2003

Westinghouse Savannah River Company
Aiken, SC 29808

Prepared for the U. S. Department of Energy under Contract DE-AC09-96SR18500 (mod. 68)

This document was prepared in conjunction with work accomplished under Contract No. DE-AC09-96SR18500 with the U. S. Department of Energy.

DISCLAIMER

This report was prepared as an account of work sponsored by an agency of the United States Government. Neither the United States Government nor any agency thereof, nor any of their employees, makes any warranty, express or implied, or assumes any legal liability or responsibility for the accuracy, completeness, or usefulness of any information, apparatus, product or process disclosed, or represents that its use would not infringe privately owned rights. Reference herein to any specific commercial product, process or service by trade name, trademark, manufacturer, or otherwise does not necessarily constitute or imply its endorsement, recommendation, or favoring by the United States Government or any agency thereof. The views and opinions of authors expressed herein do not necessarily state or reflect those of the United States Government or any agency thereof.

This report has been reproduced directly from the best available copy.

Available for sale to the public, in paper, from: U.S. Department of Commerce, National Technical Information Service, 5285 Port Royal Road, Springfield, VA 22161,
phone: (800) 553-6847,
fax: (703) 605-6900
email: orders@ntis.fedworld.gov
online ordering: <http://www.ntis.gov/help/index.asp>

Available electronically at <http://www.osti.gov/bridge>
Available for a processing fee to U.S. Department of Energy and its contractors, in paper, from: U.S. Department of Energy, Office of Scientific and Technical Information, P.O. Box 62, Oak Ridge, TN 37831-0062,
phone: (865)576-8401,
fax: (865)576-5728
email: reports@adonis.osti.gov

Table of Contents

Summary	1
Introduction	1
Model Development	3
Experimental Design	5
Experimental	6
Results	7
Discussion	15
Conclusions	17
References	18

List of Tables

Table 1. Pitzer Multielectrolyte Eq. Parameters for Ternary Systems.....	8
Table 2. NaNO ₃ Solution Preparation	9
Table 3. NaBF ₄ Solution Preparation	9
Table 4. KNO ₃ Solution Preparation	10
Table 5. Boron and Potassium Concentrations at 25°C	11
Table 6. Solubility Products and Activity Coefficients at 25°C.....	13
Table 7. KBF ₄ Hydrolysis Experiments.....	14
Table 8. KBF ₄ Solubility Data based on ICP Experimental Results, Molal Basis	14
Table 9. Summary Comparisons at Ionic Strength of Saturation, No Added Salt.....	14
Table 10. KBF ₄ Saturation Experiments in SRS Plant Solutions	17
Table 11. Modeling Results for KBF ₄ Experiments, 20°C	17

List of Figures

Figure 1. Pitzer Coefficients for NaNO ₃ Single Slat Equation.....	5
Figure 2. Solubility Product of KBF ₄ in Ionic Strength Adjuster Salts, 25°C.....	12
Figure 3. Activity Coefficient of KBF ₄ in Ionic Strength Adjuster Salts, 25°C.....	12
Figure 4. Pitzer-Kim Linear Eq. 9 Plot for KBF ₄ in NaNO ₃ ionic Strength Adjuster Showing Non-Linear Effect.....	16

Use of Modeling for the Prevention of Solids Formation during Canyon Processing of Legacy Nuclear Materials

Summary

The Department of Energy's (DOE) Environmental Management (EM) nuclear material stabilization program at the Savannah River Site (SRS) includes the dissolution and processing of legacy materials from various DOE sites. The SRS canyon facilities were designed to dissolve and process spent nuclear fuel and targets. As the processing of typical materials is completed, unusual and exotic nuclear materials are being targeted for stabilization. These unusual materials are often difficult to dissolve using historical flowsheet conditions and require more aggressive dissolver solutions. As such, solids must be prevented in the dissolver to avoid expensive delays associated with the build-up of insoluble material in downstream process equipment. Moreover, it is vital to prevent precipitation of all solids, especially plutonium-bearing solids and soluble neutron poisons, since their presence in dissolver solutions raises nuclear criticality safety issues. To prevent precipitation of undesirable solids in SRS aqueous process solutions, accurate computer models (incorporating plant specific fundamental data) are necessary.

Basic chemical data (solubility products and activity coefficients) applicable to the prevention of KBF_4 precipitation, with key binary and ternary interaction parameters considered, were obtained. Increasing the ionic strength was found to increase the solubility of KBF_4 substantially. This important observation suggests that plant solutions will be able to tolerate higher concentrations of boron than predicted without the incorporation of actual activity coefficients in model calculations. Incorporation of these data into the Idaho National Engineering and Environmental Laboratory (INEEL) speciation program, previously developed to calculate individual component concentrations in acidic aqueous fluoride systems will contribute to the application of the program (via the Pitzer correlation) to derive accurate SRS-specific activity coefficient parameters. Consequently, accurate predictions of solubilities of potentially precipitating species in plant solutions will be possible along with the ability to calculate solution adjustments to assure stability (prevent precipitation of unwanted species). The computer program will have potential applications at all DOE sites working with EM materials in aqueous solutions.

Introduction

To successfully model complex electrolyte systems, the following must be considered: 1) solution reactions and speciation, 2) reaction equilibrium constants, 3) activity coefficients of ionic, molecular, and solvent species, 4) reference states and properties at the reference state for ionic, salt, molecular, and solvent species, and 5) thermodynamic properties.¹ The complexity of an electrolyte solution is due mainly to ionic speciation via dissociation, association, and salt precipitation reactions. The complex task of determining the extent a species exists under plant conditions involves solving a set of nonlinear equations for chemical equilibrium, and requires accurate reaction equilibrium constants and activities for all the species. The Pitzer^{2,3} or the

electrolyte Non-Random Two Liquid (NRTL) model⁴ may be applied to derive the activity coefficients. These are widely used models; parameters have been extensively tabulated for various salts and acids.

As a result of processing naval nuclear fuels at the Idaho Nuclear Technology and Engineering Center (INTEC), the Idaho National Engineering and Environmental Laboratory (INEEL) developed expertise in aqueous fluoride chemistry. This process included nuclear material dissolution in hydrofluoric and nitric acids and incorporated boron as a soluble neutron poison for criticality control. The need to keep boron and other species soluble required development of a thermodynamic speciation program, for predicting multiple fluoride species equilibrium concentrations in representative plant solutions. In recent years, the INEEL modeling capability has been expanded with the incorporation of complexation equilibrium calculations into a free energy minimization program with a database for over 15,000 compounds. To apply the INEEL model to a new application, the user must incorporate plant specific data for the performance of activity coefficient (via Pitzer model application) and phase equilibrium calculations. For application to multielectrolyte solutions, data for both single and binary salt solutions are required to obtain ion interaction parameters for all ions in solution.

Research and development pertaining to SRS canyon dissolver precipitation issues was important during the Sand, Slag, and Crucible (SS&C) campaign of 1997. During the flowsheet development for this campaign, high concentrations of potassium fluoride in the boric acid-nitric acid dissolver solution resulted in white solids. These solids were identified as potassium tetrafluoroborate (KBF₄), indicating a decrease in soluble boron, a neutron adsorbing poison required for nuclear criticality control. The conditions that shift the equilibrium towards precipitation are qualitatively understood in terms of Le Chatelier's principle by considering the following equation:



As a result of the SS&C campaign issues, the INEEL model was used to predict nuclear material residue dissolution using calcium fluoride in the presence of boric acid and to predict the corrosion potential of the stainless steel dissolver vessel.⁵ However, the INEEL speciation program thermodynamic data are applicable at ionic strengths of INEEL process solutions; it did not possess activity coefficients applicable to SRS plant solutions. Therefore, application to SRS solutions with high ionic strength required that the INEEL model be improved with specific information on chemical species, such as activity coefficients and interaction parameters. Accordingly, the present study reports on the enhancement of the INEEL speciation computer program with new basic chemical data in order to better predict and avoid precipitation of undesirable solids in SRS aqueous process solutions. This incorporation will enable accurate predictions of solubilities of potentially precipitating species in plant solutions and provide the ability to calculate solution adjustments to assure stability.

Model Development

For application of the INEEL (Pitzer) model to multielectrolyte solutions, data from both single salt and binary salt solutions are required to obtain ion-interaction parameters for all ions in solution. To this end, activity coefficients as a function of ionic strength were determined by KBF_4 solubility measurements at various ionic strengths. Specifically, the determination of KBF_4 binary and ternary activity coefficient parameters was based on KBF_4 solubility measurements as a function of the ionic strength of an adjuster salt (NaNO_3 , NaBF_4 , and KNO_3). The fluoroborate ion (BF_4^-) hydrolyzes slightly to yield H_3BO_3 and HF . Therefore, chemical additions (small amounts of HF and H_3BO_3 at levels that did not contribute to ion interactions) were made to the test solutions, preventing hydrolysis of BF_4^- that would otherwise occur to about 3.7%.⁶ These data, along with literature values of Pitzer parameters for interactions of $\text{Na}^+ - \text{NO}_3^-$, $\text{K}^+ - \text{NO}_3^-$, $\text{Na}^+ - \text{BF}_4^-$, and $\text{K}^+ - \text{Na}^+$ enabled evaluation of all pertinent two-salt interaction parameters yielding KBF_4 activity coefficients as a function of ionic strength.

The following description is developed in terms of individual ions of a salt being characterized, rather than simple solubility of the pure salt, so that solubility product can be expressed when the salt is in the presence of an ionic strength adjuster with a common ion. Once the salt solubilities have been determined as a function of ionic strength, the activity coefficients are calculated as follows. For the general salt dissolution, Eq. (2), the molal concentration equilibrium constant (solubility product, K_m) and thermodynamic equilibrium constant, K_{Th} , are obtained by Eqs. (3) and (4).



$$K_m = m_{\text{A}^{z^+}}^x m_{\text{B}^{z^-}}^y \quad (\text{Eq. 3})$$

$$K_{\text{Th}} = a_{\text{A}^{z^+}}^x a_{\text{B}^{z^-}}^y = K_m \gamma_{\pm}^v \quad (\text{Eq. 4})$$

where, m is the molal concentration, a is the activity, γ_{\pm} is the mean molal activity coefficient $[(\gamma_{\text{A}^{z^+}}^x \gamma_{\text{B}^{z^-}}^y)^{1/v}]$, and v is $x + y$. Let $K_{m,0}$ and γ_0 be initially the solubility product (molal) and the mean activity coefficient, respectively, of the salt in pure water and K_m and γ_{\pm} be the corresponding values in a solution with added electrolyte that increases the ionic strength, I [$I = \frac{1}{2} \sum_i m_i z_i^2$, in the present case, $I = \frac{1}{2} (m_{\text{A}^{z^+}} z_+^2 + m_{\text{B}^{z^-}} z_-^2)$]. Then,

$$K_{\text{Th}} = K_{m,0} \gamma_0^v = K_m \gamma_{\pm}^v \quad (\text{Eq. 5})$$

so that $K_m \gamma_{\pm}^v = K_{m,0} \gamma_0^v$. Taking logarithms, we have

$$\log K_m = \log (K_{m,0} \gamma_0^v) - \log \gamma_{\pm}^v \quad (\text{Eq. 6})$$

Once $K_{m,0}\gamma_0^v$ is known, the activity coefficient at a given ionic strength can be calculated from the measured solubility product. To obtain $K_{m,0}\gamma_0^v$, $\log K_m$ is plotted against $I^{1/2}$. The plot is extrapolated to $I^{1/2} = 0$. The intercept gives $K_{m,0}\gamma_0^v$ at zero ionic strength, where $\gamma_0 = 1$. Then, from the measured solubility product at each ionic strength, Eq. (5) is solved for γ_{\pm} .

$$\gamma_{\pm} = \left(\frac{K_{m,0}\gamma_0^v}{K_m} \right)^{1/v} \quad (\text{Eq. 7})$$

The form of the suggested extrapolation equation arises from the limiting Debye-Hückel law, which predicts a linear relation between $\log \gamma_{\pm}$ and $I^{1/2}$ at very low ionic strengths. This method is valid only up to a few hundredths molal and was not used.

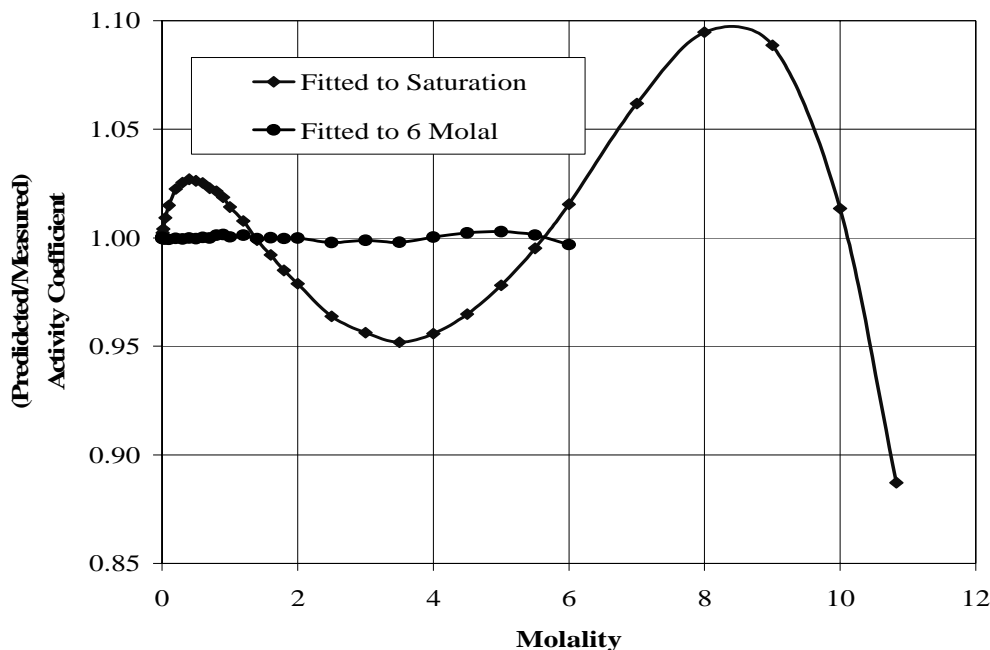
A better extrapolation plot was applied herein⁷ and used an extended Debye-Hückel equation developed by Davies⁸:

$$\log K_m - \frac{A_{\gamma}\Delta z^2 I^{1/2}}{1 + I^{1/2}} = \log K_{m,0} + bI \quad (\text{Eq. 8})$$

where A_{γ} , the Debye-Hückel limiting slope, is 0.511 at 25°C and Δz^2 is $\Sigma(z_{products})^2 - (z_{reactants})^2$. The left side was plotted against I and extrapolated to zero I , yielding $\log K_{m,0}$ at the intercept. The $K_{m,0}$ value was determined from the lower ionic strength data, and activity coefficients at all ionic strengths were evaluated from Eq. (7) with $\gamma_0 = 1$. Although, Phillips et al. applied this function to evaluate solubility products at zero ionic strength from data up to 3 molal ionic strength,⁷ the function was originally developed by fitting data below about 0.15 molal.⁸ Thus, precise data exhibits curvature above 0.25 molal, evidenced by results obtained herein for KBF_4 in sodium nitrate (NaNO_3). Consequently, only data up to 0.25 molal ionic strength were used for the linear extrapolation to zero ionic strength.

An initial assessment of the Pitzer model was performed based on literature data and calculating individual activity coefficients at experimental conditions. This demonstrated that, when fitting the data up to 6 molal, the Pitzer model calculated the activity coefficients with an accuracy of 0.3%. For data above 6-molal, the effect on the fitting accuracy of the overall data must be considered on a case-by-case basis. Figure 1 shows the prediction capability of Pitzer single-salt equation parameters for NaNO_3 activity coefficients.⁹

Upon determination of individual species activity coefficients, plant solution stability is provided via application of the HSC program, a commercial free energy minimization program (HSC Chemistry[®] for Windows).¹⁰ The INEEL model possesses general equations and methodology to convert equilibrium constants into a consistent set of thermodynamic parameters for use in the HSC program. As a result, solution compositions can be varied to determine concentration limits where precipitation occurs.

Figure 1. Pitzer Coefficients for NaNO_3 Single Salt Equation.

Experimental Design

The experimental design to determine critical ion interaction parameters for ion pairs is shown in Table 1. For the $\text{KBF}_4 - \text{NaNO}_3$ system (no common ion), the θ and ψ parameters were obtained from the $\text{KBF}_4 - \text{NaBF}_4$ and $\text{KBF}_4 - \text{KNO}_3$ systems. Then, the $\text{K}^+ - \text{BF}_4^-$ parameters of $\beta^{(0)}$, $\beta^{(1)}$, and C^ϕ to high ionic strength were obtained with this system. For the $\text{KBF}_4 - \text{NaBF}_4$ system (common anion), ψ was assumed for $\text{K}^+ - \text{Na}^+ - \text{BF}_4^- = -0.002$, similar to that for $\text{K}^+ - \text{Na}^+ - \text{Cl}^-$, $\text{K}^+ - \text{Na}^+ - \text{Br}^-$, and $\text{K}^+ - \text{Na}^+ - \text{NO}_3^-$. K^+ solubility concentration was measured as function of NaBF_4 added concentration. $[\text{KBF}_4]$ varies dramatically with $[\text{NaBF}_4]$, so its parameters are easily attainable. Data up to 0.2 to 0.4 m NaBF_4 is reasonable, at which $[\text{KBF}_4]$ was expected to have decreased to about 0.0088 m and $[\text{K}^+]/[\text{BF}_4^-]$ to 0.042. (In practice, data up to 2.5 m KBF_4 was obtained, as the solubility increased as a result of activity coefficients being greater than unity.) This system has the advantage over the $\text{KBF}_4 - \text{KNO}_3$ system in that the interaction parameter for $\text{K}^+ - \text{Na}^+$ is known, whereas for $\text{BF}_4^- - \text{NO}_3^-$ it is not. This system was used to get the $\text{K}^+ - \text{BF}_4^-$ parameters. Then, the $\text{KBF}_4 - \text{KNO}_3$ system, was used to get the $\text{BF}_4^- - \text{NO}_3^-$ θ parameter. These two systems were also used to determine the ψ parameters. The limitation of this system, and the next, is that the KBF_4 activity coefficient will not be obtained at high ionic strength. Therefore, the $\text{KBF}_4 - \text{NaNO}_3$ system was applied to extend the $\text{K}^+ - \text{BF}_4^-$ parameter determinations to high ionic strength. For the $\text{KBF}_4 - \text{KNO}_3$ system, BF_4^- solubility concentration was measured as function of KNO_3 concentration. $[\text{KBF}_4]$ varies dramatically with $[\text{KNO}_3]$, so parameter attainment was straightforward. Data was expected to be obtained up to 0.2 to 0.4 m

KNO_3 , where $[\text{KBF}_4]$ was anticipated to have decreased to about 0.0088 m and $[\text{K}^+]/[\text{BF}_4^-]$ to 0.042. Again, increased solubilities countering the common ion effect enabled data collection to 2.5 m KNO_3 .

Experimental

The solubility of KBF_4 was determined as a function of ionic strength in three matrixes: NaNO_3 , KNO_3 , and NaBF_4 . To this end, a series of electrolyte solutions (NaNO_3 , NaBF_4 , and KNO_3) was prepared as illustrated in Tables 2, 3, and 4. From each original solution, three additional solutions were prepared with successively increasing spikes of KBF_4 . These solutions were analyzed for boron and potassium by ICP-ES. Consequently, each original solution was represented by a three-point graph of both boron and potassium concentrations. These graphs were extrapolated back to zero spike addition to ascertain boron and potassium concentrations of the original solution. This multiple successive standard spike addition method was applied to calibrate the ICP in the experimental matrix by removing all effects except changing the BF_4^- concentration.

The solubility measurements were performed at $25.0 \pm 0.5^\circ\text{C}$. These solutions were allowed to equilibrate (mild agitation) at $25 \pm 0.5^\circ\text{C}$ for 14 days prior to sample initiation. The concentrations of B and K were determined (ICP-ES) from three series of dilutions. Materials used were KBF_4 (Aldrich, anhydrous, 99.95+%), H_3BO_3 (Aldrich, 99.5%), HF (Optima, 49%), and purified Millipore water (to $\sim 17 \text{ M ohm}$). Samples were obtained with syringe filters, 25 mm GD/X disposable, 25-mm diameter, 0.2-micrometer pore size (Whatman, Inc.) The experimental apparatus (constant temperature shaker water bath) provided accurate temperature control and efficient sampling for solubility determinations. The KBF_4 solutions were analyzed for B and K concentration by inductively couple plasma-atomic emission spectroscopy (ICP-ES). The solubility at zero ionic strength was determined by a Phillips linear plot (Eqn. 8) of data up to 0.3 molal ionic strength. From this value, the activity coefficient of KBF_4 was determined from solubility measured at each ionic strength. These data are required input to the activity coefficient model to determine the Pitzer parameters.

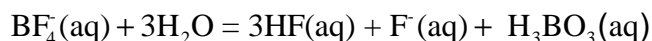
Quantitative evaluations were made of chemical adjustments to make to the KBF_4 test solutions to prevent hydrolysis of BF_4^- to less than 1% that would otherwise occur to about 3.7%; this involved small additions of HF and H_3BO_3 at levels that did not contribute to ion interactions. The KBF_4 solubility measurements for activity coefficient determinations were made in one set of experiments using NaNO_3 as an ionic strength adjuster. Interpretation of the data was based on the assumption that Na^+ and BF_4^- ions do not interact to form a complex in solution, which would cause the solubility of KBF_4 to increase. Literature information supports this assumption, i.e., no mention is found of the existence of a complexation between the ions.

A special set of tests was also conducted that investigated KBF_4 hydrolysis. Specifically, the hydrolysis of KBF_4 was determined in a pure KBF_4 aqueous solution, a second solution with the same concentration of H_3BO_3 and HF as in the above tests, and a

final solution with an excess of these constituents. These solutions were also held to $25.0 \pm 0.5^\circ\text{C}$. Table 7 provides the solution make-up concentrations.

Results

Characterizations of the three electrolyte solutions, NaNO_3 , NaBF_4 , and KNO_3 , are provided in Tables 2, 3, and 4 respectively. The equilibrium BF_4^- and K^+ concentrations along with BF_4^- hydrolysis are shown in Table 5 and Figures 2 and 3. The small residual hydrolysis was calculated and subtracted from the initial BF_4^- concentration to obtain the equilibrium concentration using the INEEL speciation program, which included thermodynamic data¹¹ for evaluating the equilibrium constant (6.41×10^{-12} at 25°C) for the hydrolysis reaction



(compared to the value of 1.0×10^{-11} of Ryss and Donskaya¹²). In the NaNO_3 system, the boron and potassium concentrations were independently measured using ICP-ES. In the NaBF_4 system, the potassium was directly measured and the BF_4^- (before hydrolysis) was calculated as the sum of the accurately measured (by weight) NaBF_4 concentration and the potassium concentration. In the KNO_3 system, the boron was directly measured and the K^+ was calculated as the sum of the accurately measured (by weight) KNO_3 and the BF_4^- (before hydrolysis).

The resultant solubility products and activity coefficients are shown in Table 6. Table 7 shows the results of the gravimetric hydrolysis experiments. Table 8 illustrates the KBF_4 solubility data, based on ICP experimental results, on a molal basis at 25°C . It should be noted that the literature data are assumed to be at the ionic strength of saturation – there is no discernment of data as a function of ionic strength with an extrapolation to zero ionic strength. Finally, Table 9 provides a summary comparison of the solubility data at ionic strength of saturation, no added salt, 25°C . The activity coefficients were calculated with the use of the ICP data (scatter of 5 to 10%) in combination with the K_{SP} extrapolated (Davies equation) to zero ionic strength, $K_{\text{SP}}^0 = 0.00267$, which corresponds to the K_{SP} value at saturation, no added salt, of 0.00368.

Table 1.
Pitzer Multielectrolyte Eq. Parameters for Ternary Systems (Two Salts + Water)

√ = parameter known from literature

– = not applicable

x = parameter needed

KBF₄ – NaNO₃ System (No Common Ion)

Interacting Ions	Single Salt Parameters			Two-Salt Parameters	
	$\beta^{(0)}$	$\beta^{(1)}$	C^ϕ	θ	ψ
Na ⁺ – NO ₃ [–]	√	√	√	–	–
K ⁺ – NO ₃ [–]	√	√	√	–	–
Na ⁺ – BF ₄ [–]	√	√	√	–	–
K ⁺ – BF ₄ [–]	x	x	x	–	–
K ⁺ – Na ⁺	–	–	–	√	–
BF ₄ [–] – NO ₃ [–]	–	–	–	x	–
BF ₄ [–] – NO ₃ [–] – K ⁺	–	–	–	–	x
BF ₄ [–] – NO ₃ [–] – Na ⁺	–	–	–	–	x
K ⁺ – Na ⁺ – NO ₃ [–]	–	–	–	–	√
K ⁺ – Na ⁺ – BF ₄ [–]	–	–	–	–	x

KBF₄ – NaBF₄ System (Common Anion)

Interacting Ions	Single Salt Parameters			Two-Salt Parameters	
	$\beta^{(0)}$	$\beta^{(1)}$	C^ϕ	θ	ψ
Na ⁺ – BF ₄ [–]	√	√	√	–	–
K ⁺ – BF ₄ [–]	x	x	x	–	–
K ⁺ – Na ⁺	–	–	–	√	–
K ⁺ – Na ⁺ – BF ₄ [–]	–	–	–	–	x

KBF₄ – KNO₃ System (Common Cation)

Interacting Ions	Single Salt Parameters			Two-Salt Parameters	
	$\beta^{(0)}$	$\beta^{(1)}$	C^ϕ	θ	ψ
K ⁺ – NO ₃ [–]	√	√	√	–	–
K ⁺ – BF ₄ [–]	x	x	x	–	–
K ⁺ – Na ⁺	–	–	–	√	–
BF ₄ [–] – NO ₃ [–]	–	–	–	x	–
BF ₄ [–] – NO ₃ [–] – K ⁺	–	–	–	–	x

Table 2.
NaNO₃ Solution Preparation

NaNO ₃ target molality	Density	Material Used for Solution				Solution Characterization					
		Water	H ₃ BO ₃	HF 25 M	NaNO ₃	NaNO ₃		HF		H ₃ BO ₃	
m	g/mL	gram	grams	μ liters	grams	M	molality	M	molality	M	molality
0.00	1.001	100.175	0.0161	21	0	0	0	0.00510	0.00513	0.00258	0.00260
0.05	1.004	100.288	0.0164	21	0.429	0.0499	0.0503	0.00508	0.00513	0.00262	0.00265
0.10	1.007	100.298	0.0166	21	0.855	0.0993	0.100	0.00508	0.00513	0.00265	0.00268
0.20	1.013	100.354	0.0165	21	1.712	0.198	0.201	0.00506	0.00512	0.00263	0.00266
0.50	1.030	100.346	0.0159	21	4.244	0.486	0.498	0.00501	0.00512	0.00251	0.00256
1.00	1.056	100.399	0.0167	21	8.502	0.959	0.996	0.00493	0.00512	0.00259	0.00269
1.50	1.082	100.169	0.0160	21	12.766	1.421	1.500	0.00486	0.00513	0.00245	0.00259
2.00	1.106	100.330	0.0165	21	17.158	1.876	2.012	0.00478	0.00513	0.00248	0.00266
2.50	1.129	100.245	0.0165	21	21.414	2.305	2.513	0.00470	0.00513	0.00244	0.00266
3.00	1.151	100.119	0.0160	21	25.656	2.721	3.015	0.00464	0.00514	0.00233	0.00259
3.50	1.172	100.176	0.0164	21	29.960	3.125	3.519	0.00456	0.00513	0.00235	0.00265
4.00	1.192	100.212	0.0167	21	34.120	3.501	4.006	0.00448	0.00513	0.00236	0.00270
5.00	1.227	100.686	0.0167	21	42.519	4.207	4.968	0.00432	0.00511	0.00227	0.00268
6.00	1.264	100.552	0.0167	21	51.097	4.912	5.979	0.00420	0.00511	0.00221	0.00269
7.00	1.300	100.168	0.0167	21	60.182	5.621	7.069	0.00408	0.00513	0.00215	0.00270
8.00	1.329	100.294	0.0167	21	68.791	6.232	8.070	0.00396	0.00513	0.00208	0.00269
9.00	1.354	100.282	0.0164	21	76.969	6.785	9.030	0.00385	0.00513	0.00199	0.00265

Table 3.
NaBF₄ Solution Preparation

NaBF ₄ target molality	Density	Material Used for Solution				Solution Characterization					
		Water	H ₃ BO ₃	HF 25 M	NaNO ₃	NaBF ₄		HF		H ₃ BO ₃	
m	g/mL	gram	grams	μ liters	grams	M	molality	M	molality	M	molality
0	1.001	100.248	0.0164	22	0	0.000	0	0.00509	0.00513	0.00258	0.00260
0.05	1.003	100.280	0.0141	18	0.5509	0.050	0.050	0.00448	0.00451	0.00226	0.00228
0.10	1.006	100.191	0.0112	14	1.1001	0.099	0.100	0.00347	0.00350	0.00179	0.00181
0.20	1.012	100.307	0.0042	5.4	2.1946	0.197	0.199	0.00133	0.00135	0.00067	0.00068
0.30	1.018	100.169	0	0	3.2357	0.290	0.294	0	0	0	0
0.40	1.024	100.124	0	0	4.4135	0.393	0.402	0	0	0	0
0.50	1.031	100.279	0	0	5.4934	0.487	0.499	0	0	0	0
1.00	1.062	100.227	0	0	11.0396	0.959	1.003	0	0	0	0
1.50	1.091	100.280	0	0	16.4896	1.402	1.498	0	0	0	0
2.00	1.120	100.307	0	0	22.0672	1.837	2.004	0	0	0	0
2.50	1.147	100.341	0	0	27.6421	2.253	2.509	0	0	0	0

Table 4.
KNO₃ Solution Preparation

KNO ₃ target molality	Density	Material Used for Solution				KNO ₃		HF		H ₃ BO ₃	
		Water	H ₃ BO ₃	HF 25 M	KNO ₃	M	molality	M	molality	M	molality
m	g/mL	gram	grams	μ liters	grams	M	molality	M	molality	M	molality
0.00	1.0012	100.405	0.0163	21	0.0000	0	0	0.0051	0.0051	0.0026	0.0026
0.05	1.0030	100.511	0.0177	22	0.4980	0.0486	0.0490	0.0054	0.0055	0.0028	0.0029
0.10	1.0061	100.195	0.0179	23	1.0773	0.1053	0.1064	0.0056	0.0057	0.0029	0.0029
0.20	1.0117	100.282	0.0195	25	2.0921	0.2037	0.2063	0.0060	0.0061	0.0031	0.0031
0.30	1.0171	100.301	0.0189	24	3.0613	0.2969	0.3019	0.0058	0.0059	0.0030	0.0030
0.40	1.0230	100.288	0.0192	25	4.0677	0.3929	0.4012	0.0060	0.0061	0.0030	0.0031
0.50	1.0286	100.140	0.0192	25	5.0842	0.4899	0.5022	0.0060	0.0061	0.0030	0.0031
1.00	1.0566	100.349	0.0196	25	10.1423	0.9565	0.9997	0.0058	0.0061	0.0030	0.0032
1.50	1.0830	100.374	0.0194	25	15.1772	1.4025	1.4956	0.0057	0.0061	0.0029	0.0031
2.00	1.1077	100.295	0.0195	25	20.2544	1.8358	1.9974	0.0056	0.0061	0.0029	0.0031
2.50	1.1316	100.359	0.0194	25	25.3113	2.2524	2.4945	0.0055	0.0061	0.0028	0.0031

Table 5.
Boron and Potassium Concentrations at 25°C

Electrolyte		Equilibrium BF ₄ ⁻ molality*	BF ₄ ⁻ Hydrolysis molality	K molality
Species	molality			
NaNO ₃	0.0000	0.0585	0.00047	0.0640
NaNO ₃	0.0503	0.0638	0.00051	0.0684
NaNO ₃	0.1003	0.0656	0.00052	0.0695
NaNO ₃	0.2007	0.0720	0.00052	0.0726
NaNO ₃	0.4976	0.0836	0.00066	0.0863
NaNO ₃	0.9963	0.0987	0.00074	0.105
NaNO ₃	1.4996	0.107	0.00079	0.116
NaNO ₃	2.0121	0.119	0.00084	0.125
NaNO ₃	2.5134	0.135	0.00093	0.144
NaNO ₃	3.0150	0.149	0.00101	0.152
NaNO ₃	3.5157	0.161	0.00104	0.166
NaNO ₃	4.0039	0.186	0.00115	0.180
NaNO ₃	4.9984	0.210	0.00124	0.212
NaNO ₃	5.9788	0.235	0.00113	0.231
NaNO ₃	7.0688	0.260	0.00141	0.265
NaNO ₃	8.0698	0.275	0.00146	0.283
NaNO ₃	9.0302	0.275	0.00147	0.279
NaBF ₄	0.0000	0.0585	0.00047	0.0640
NaBF ₄	0.0500	0.0897	0.00087	0.0405
NaBF ₄	0.1000	0.128	0.00136	0.0289
NaBF ₄	0.1993	0.217	0.00234	0.0199
NaBF ₄	0.2942	0.309	0.00302	0.0182
NaBF ₄	0.4015	0.416	0.00328	0.0179
NaBF ₄	0.4989	0.511	0.00349	0.0158
NaBF ₄	1.0032	1.010	0.00431	0.0115
NaBF ₄	1.4977	1.506	0.00494	0.0130
NaBF ₄	2.0037	2.011	0.00548	0.0128
NaBF ₄	2.5091	2.518	0.00602	0.0155
KNO ₃	0.0000	0.0585	0.00047	0.0640
KNO ₃	0.0490	0.0447	0.00024	0.0941
KNO ₃	0.1064	0.0385	0.00013	0.145
KNO ₃	0.2063	0.0295	-0.00009	0.236
KNO ₃	0.3019	0.0282	-0.00062	0.329
KNO ₃	0.4012	0.0300	-0.00008	0.431
KNO ₃	0.5022	0.0268	-0.00013	0.530
KNO ₃	0.9997	0.0236	-0.00017	1.023
KNO ₃	1.4956	0.0271	-0.00012	1.522
KNO ₃	1.9974	0.0250	-0.00015	2.018
KNO ₃	2.4945	0.0233	-0.00017	2.463

*Measured or derived boron concentration corrected for added H₃BO₃ (subtracted) and after subtracting BF₄⁻ hydrolysis, next column.

Figure 2. Solubility Product of KBF_4 in Ionic Strength Adjuster Salts, 25°C
Addition of Salts Increases Solubility

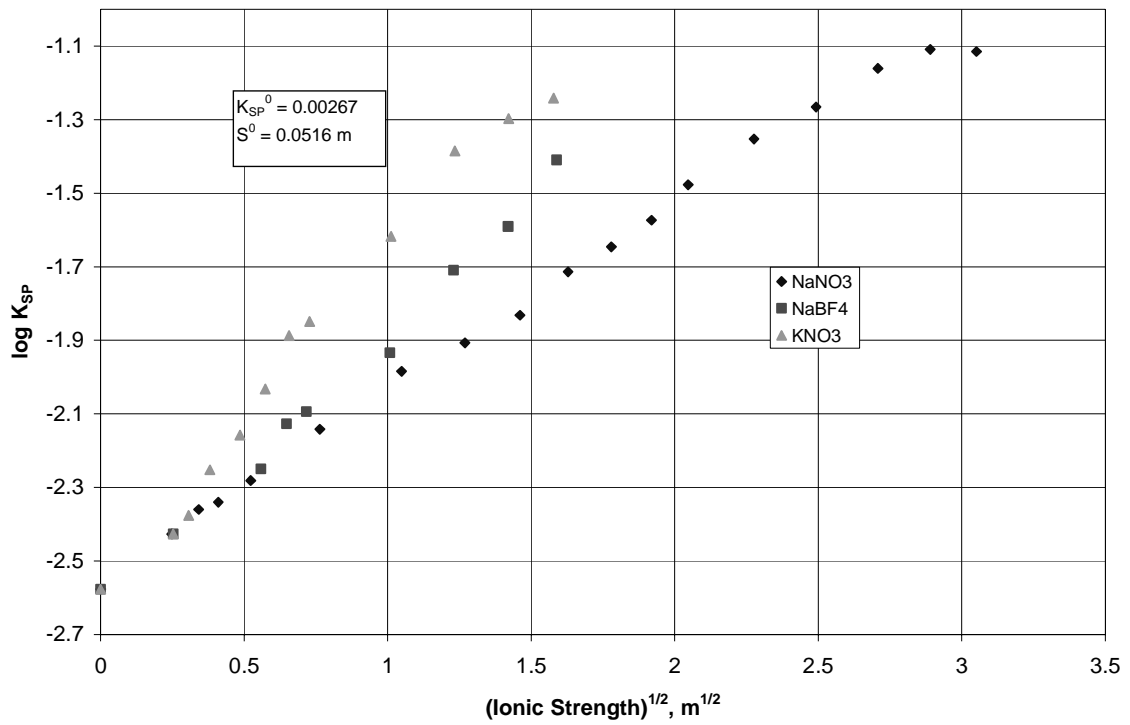


Figure 3. Activity Coefficient of KBF_4 in Ionic Strength Adjuster Salts, 25°C

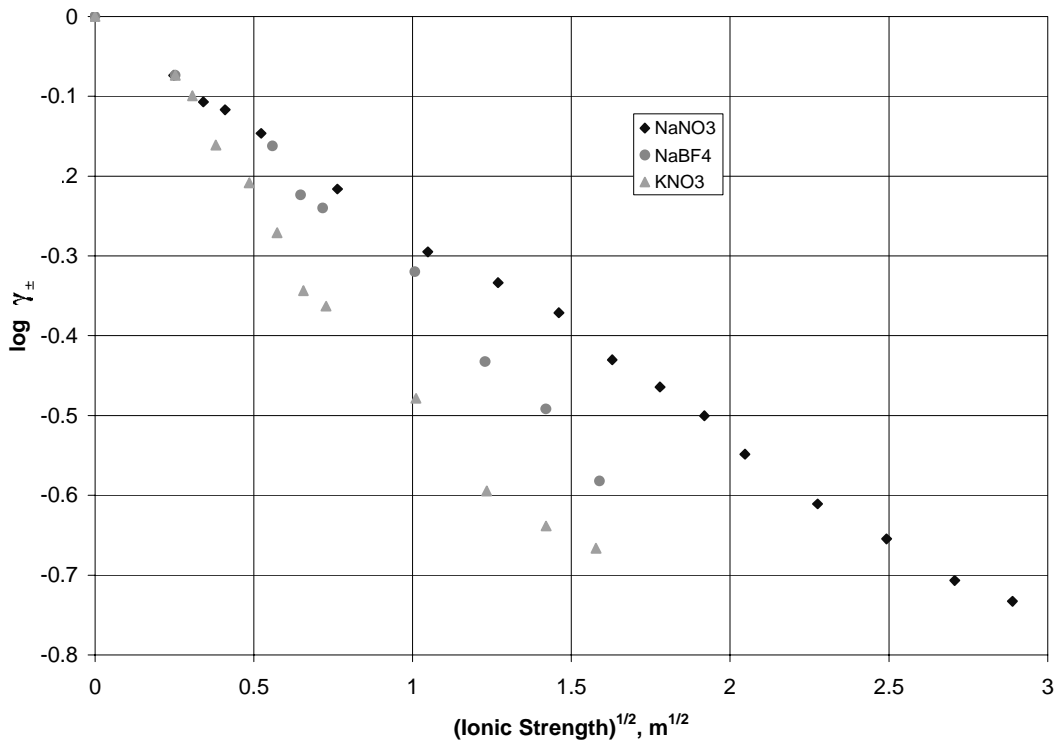


Table 6.
KBF₄ Solubility Products and Activity Coefficients at 25°C

Electrolyte	m	K _{SP}	Ionic Strength	Mean Molal Activity Coefficient
NaNO ₃	0.0000	0.00375	0.0640	0.844
NaNO ₃	0.0503	0.00436	0.1167	0.781
NaNO ₃	0.1003	0.00456	0.1681	0.764
NaNO ₃	0.2007	0.00523	0.2733	0.714
NaNO ₃	0.4976	0.00721	0.5829	0.608
NaNO ₃	0.9963	0.0104	1.099	0.507
NaNO ₃	1.4996	0.0124	1.611	0.464
NaNO ₃	2.0121	0.0147	2.134	0.425
NaNO ₃	2.5134	0.0193	2.653	0.371
NaNO ₃	3.0150	0.0226	3.166	0.343
NaNO ₃	3.5157	0.0267	3.683	0.316
NaNO ₃	4.0039	0.0333	4.189	0.283
NaNO ₃	4.9984	0.0444	5.180	0.245
NaNO ₃	5.9788	0.0543	6.213	0.222
NaNO ₃	7.0688	0.0690	7.332	0.196
NaNO ₃	8.0698	0.0778	8.350	0.185
NaNO ₃	9.0302	0.0767	9.308	0.186
NaBF ₄	0.0000	0.00375	0.0640	0.844
NaBF ₄	0.0500	0.00363	0.0905	0.857
NaBF ₄	0.1000	0.00369	0.1289	0.850
NaBF ₄	0.1993	0.00432	0.2192	0.785
NaBF ₄	0.2942	0.00563	0.3124	0.688
NaBF ₄	0.4015	0.00746	0.4194	0.598
NaBF ₄	0.4989	0.00804	0.5147	0.575
NaBF ₄	1.0032	0.0116	1.015	0.479
NaBF ₄	1.4977	0.0195	1.511	0.369
NaBF ₄	2.0037	0.0256	2.016	0.322
NaBF ₄	2.5091	0.0389	2.524	0.262
KNO ₃	0.0000	0.00375	0.0640	0.844
KNO ₃	0.04900	0.00421	0.0942	0.796
KNO ₃	0.1064	0.00559	0.1451	0.690
KNO ₃	0.2063	0.00696	0.2357	0.619
KNO ₃	0.3019	0.00928	0.3291	0.536
KNO ₃	0.4012	0.0130	0.4312	0.453
KNO ₃	0.5022	0.0142	0.5293	0.433
KNO ₃	0.9997	0.0241	1.023	0.332
KNO ₃	1.4956	0.0412	1.522	0.254
KNO ₃	1.9974	0.0504	2.020	0.230
KNO ₃	2.4945	0.0574	2.490	0.216

Table 7. KBF_4 Gravimetric Hydrolysis Experiments

Description	H_2O	H_3BO_3	HF	KBF_4	H_3BO_3	HF	Density	KBF_4
	g	g	μL	g	m	m	g/mL	m
Pure KBF_4	500.0	0	0	7	0	0	0.9979	0.0504
H_3BO_3 & HF (same as in present study)	500.0	0.628	102	7	0.00203	0.0051	1.0068	0.0517
Excess H_3BO_3 & HF (to stop hydrolysis)	500.0	0.631	144	7	0.00204	0.0072	1.0081	0.0529

Table 8. KBF_4 Solubility Data Based on ICP Experimental Results, Molal Basis, 25°C.

Ionic Strength Adjuster	ICP Data Extrapolated to Zero I, Davies Equation		Values at Ionic Strength of KBF_4 Saturation <i>No Added Ionic Strength Salt</i>						
			Raw Saturation Data			Calculated at I of Saturation from Davies Linear Fit Equation		Literature Values References 13, 14	
	K_{SP}^0	S^0	I	K_{SP}	S	K_{SP}^*	S^*	K_{SP}^*	S^*
NaNO_3	0.00268	0.0518	0.0615	0.00375	0.0615	0.00382	0.0620	0.00183	0.043
NaBF_4	0.00268	0.0517				0.00343	0.0588		
KNO_3	0.00289	0.0538				0.00380	0.0619		
Average	0.00275	0.0524				0.00368	0.0609	0.00380	0.062

* Corrected for hydrolysis. To the two significant figures provided in the literature, there is no difference between with and without the hydrolysis correction.

Table 9. Summary Comparisons at Ionic Strength of Saturation, No Added Salt, 25°C.

Source of Results		K_{SP}	S
Present Study	ICP Data	0.0037	0.061
	Gravimetric Data	0.0026	0.052
Literature Values	Stolba (1872) ¹³	0.0018	0.043
	DeBoer & Van Liempt (1927) ¹⁴	0.0038	0.062

Discussion

In general, electrolyte solution reactions generate additional species that substantially increase the number of possible binary and ternary parameters. The findings of the experimental program provide a foundation of basic chemical data (solubility products and activity coefficients) applicable to the prevention of KBF_4 precipitation, with key binary and ternary interaction parameters considered. An important observation is that increasing the ionic strength increases the solubility of KBF_4 substantially, which means that plant solutions will be able to tolerate higher concentrations of boron than would be estimated in the absence of activity coefficients.

Application of the INEEL speciation program to solutions characteristic of SRS dissolvers requires evaluation of activity coefficients via the Pitzer correlation parameters. To obtain the Pitzer parameters in the multielectrolyte systems, the procedure developed by Pitzer and Kim¹⁵ was followed. They developed a linear graphical procedure derived from empirical correlations for evaluation of the ternary system ion interaction parameters θ_{ij} and Ψ_{ijk}

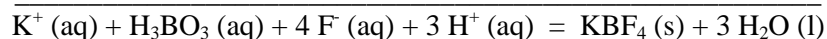
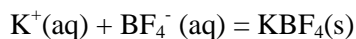
$$\Delta \ln \gamma_{MX} \left(\frac{v}{2v_M m_N} \right) = \theta_{MN} + \frac{1}{2} \left(m_X + m_M \left| \frac{z_M}{z_X} \right| \right) \Psi_{MNX} \quad (\text{Eq. 9})$$

where, m_N is the molality of the cation of the ionic strength adjuster salt. The term $\Delta \ln \gamma_{MX}$ is the difference between the experimental value of $\ln \gamma_{MX}$ with the appropriate single-salt parameters values for the pure single-electrolyte terms, but with $\theta_{MN} = \Psi_{MNX} = 0$ in the multielectrolyte activity coefficient equation. Pitzer's approach was followed: the left side of equation (9) was plotted against the coefficient of Ψ on the right side to obtain a linear plot with intercept θ and slope Ψ . This simple approach avoided the need to solve the non-linear activity coefficient equations using multiple regression. However, in the application of this approach down to small concentrations of the ionic strength adjuster salt (m_N in equation (9)), a non-linear plot resulted due to the left side approaching infinity as m_N approached zero. This is evident in Figure 4 for the NaNO_3 system using the literature value for $\theta_{\text{K-Na}}$ of -0.012 . This problem was first identified by Khoo¹⁶ and subsequently by Kim and Frederick.¹⁷ Accordingly, the data processing approach of non-linear multiple regression is appropriate and needed. This effort is in progress. Upon its completion, a journal article will be prepared of the results.

The KBF_4 solubility data (based on ICP results) compare well with previously reported values (DeBoer and Van Liempt¹⁴). The lower solubility determined via gravimetric methods is not understood. Consequently, there is a degree of uncertainty in the K_{SP}^0 and K_{SP} at saturation, no added salt based on the ICP and gravimetric comparisons. Nevertheless, the activity coefficients are valid because of the use of a self consistent set of ICP data from which the used K_{SP}^0 value was extrapolated. It is noted that the gravimetric measurements with added H_3BO_3 and HF could not discern the extent of hydrolysis.

The INEEL model was previously adapted to SRS plant dissolver solutions to support the 1997 Sand, Slag, and Crucible campaign and the Mark 42 Fuel Tube campaign. This was due to a high concentration of fluoride ions in boric acid/nitric acid solutions that led to the formation of a white solid (see Table 10). The white solids were collected from these flow sheet simulations and were identified as KBF_4 .

The conditions that shift the equilibria towards precipitation are qualitatively understood in terms of Le Chatelier's principle by considering the following equations:



Test Case 37 is just at saturation and Case 38 is over-saturated. These cases were modeled with the INEEL speciation program with the results shown in Table 11.

The model properly predicts precipitation of KBF_4 at 0.60-M fluoride but slightly overpredicts solution stability at 0.50-M fluoride. This observation may be due to a complex interaction of activity coefficients of the ions in solution and the effect of HNO_3 on activity of HF. To optimize model development, it is necessary to determine the activity coefficients of HF in HNO_3 and apply them in combination with calculated activity coefficients for the ionic species in solution. This can be done following completion of the regression fitting of the Pitzer ion interaction parameters (see Appendix). As it stands, the model can predict the KF concentration stability limit to within about 12%. This is based on the 41% of saturation predicted at 0.50 M KF and correct prediction at 0.60 M KF $[(1-0.41)*(0.60-0.50)/0.50] = 0.12$. This precision is sufficient for plant process control with safety factors.

Figure 4. Pitzer-Kim Linear Eq. 9 Plot for KBF_4 in NaNO_3 Ionic Strength Adjuster Showing Non-Linearity Effect.

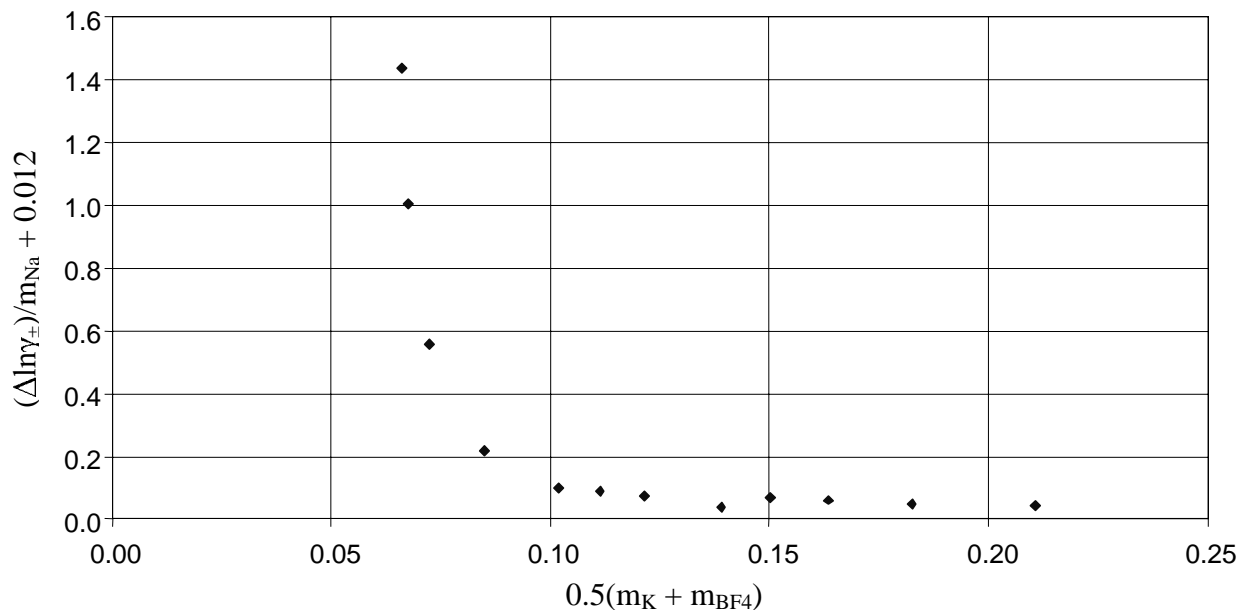


Table 10. KBF₄ Saturation Experiments in SRS Plant Solutions

Date	Test	[HNO ₃] ₀ (M)	[F ⁻] ₀ (M)	[B] ₀ (g/L)	Observation
Dec-97	SS&C-sim.	9.3	0.30	2.5	Unidentified White solid
May-98	SS&C-sim. (gelatin strike)	1.0	0.23	1.7	White solid, KBF ₄ (s)
Nov-98	SS&C-test 1	8.8	0.32	1.6	No solids
	SS&C-test 2	8.6	0.40	2.2	KBF ₄ (s)
Feb-99	Mark 42 -sim [Al] = 0.44 M				
	Test Case 36	1.0	0.40	2.5	No solids
	Test Case 37	1.0	0.50	2.5	KBF ₄ (s), few
	Test Case 38	1.0	0.60	2.5	KBF ₄ (s), some

Table 11. Modeling Results for KBF₄ Experiments, 20°C

Test Case	[HNO ₃] ₀ M	[KF] ₀ M	[B] ₀ g/L	[Al] ₀ M	Mark-42-sim Observation	Using INEEL program, Calculated:
37	1.0	0.50	2.5	0.44	KBF ₄ (s), few	[BF ₄ ⁻] = 41.2% of saturation (i.e. no precipitation is predicted).
38	1.0	0.60	2.5	0.44	KBF ₄ (s), some	Predicts saturated KBF ₄ . Precipitate composition: 1.9% of K ⁺ 7.6% of F (4.9% of F as KBF ₄)

Conclusions

With the objective of preventing precipitation of undesirable solids during aggressive SRS dissolution processes of EM materials, new basic chemical data were determined leading to a better ability to predict and avoid solids production in aqueous process solutions at SRS. The basic chemical data includes solubility, activity coefficients, and solubility products of potassium tetrafluoroborate (KBF₄) at ionic strengths expected in process solutions. These data will enhance the capability of the INEEL program to calculate the equilibrium position for a given starting dissolver solution composition and the solution stability is determined. Solution compositions can be varied to determine the concentration limit at which precipitation will begin in a dissolver solution.

This effort to develop a predictive model of the stability of aqueous solutions of nuclear materials will enable the avoidance of concentrations that may cause salts to precipitate. Therefore, for the processing of off-normal material, the risk of producing unwanted solids that require processing to stop will be reduced. Processing delays result in higher operating costs. In addition, the improved model may reduce the work scope

for future flowsheet development by identifying the concentration of dissolver solutions that avoid the precipitation of salts. As an initial impact, the improved INEEL model should reduce costs for the processing of difficult-to-dissolve residues from the Rocky Flats Environmental Technology Site by shortening the time it takes to determine dissolving solutions. As a long-term impact, this model should improve schedules to dissolve other off-normal nuclear materials and process aqueous solutions that are stored throughout the DOE complex.

References

1. Y. Liu and S. Watanasiri, *Chem. Eng. Prog.*, 25-42, October 1999.
2. K. S. Pitzer, *J. Phys. Chem.*, **77**, 268 (1973).
3. K. S. Pitzer, "Ion Interaction Approach: Theory and Data Correlation," Chapter 3 in *Activity Coefficients in Electrolyte Solutions*, 2nd Edition, K. S. Pitzer, editor, CRC Press, Boca Raton, 1991.
4. C. C. Chen, H. I. Britt, J. F. Boston, and L. B. Evans, *AIChE J.* **28** (4), 588-596, (July 1982).
5. J. D. Christian, *Dissolution of Sand, Slag, and Crucible Residues, Chemistry Modeling Considerations*, Report Prepared for Westinghouse Savannah River Company, (January 5, 1998).
6. R. F. Platford, "Osmotic and activity coefficients of simple borates in aqueous solution at 25°", *Canadian Journal of Chemistry*, **47**, 2271-2273 (1969).
7. S. L. Phillips, F. V. Hale, L. F. Silvester, and M. D. Siegel, *Thermodynamic Tables for Nuclear Waste Isolation*, Report NUREG/CR-4864/LBL-22860/SAND87-0323, Vol 1 (June 1988).
8. C. W. Davies, *Ion Association* (Butterworths, Washington, DC, 1962).
9. W. J. Hamer and Y. Wu, "Osmotic Coefficients and Mean Activity Coefficients of Uni-univalent Electrolytes in Water at 25°C," *J. Phys. Chem. Ref. Data*, Vol. 1, No. 4, 1047-1099 (1972).
10. A. Roine, Outokumpo HSC Chemistry® for Windows, Chemical Reaction and Equilibrium Software with Extensive Thermochemical Database, Version 5.1, Outokumpo Research Oy Information Service, P O Box 60, FIN-28101 Pori, Finland; available from ESM Software, Hamilton, Ohio.
11. R. R. Hammer, *A Determination of the Stability Constants of a Number of Metal Fluoride Complexes and Their Rates of Formation*, Report ENICO-1004, August 1979. National Technical Information Service, Springfield, Virginia.
12. I. G. Ryss and B. B. Donskaya, *Zh. Fiz. Khim.*, **33**, 107 (1959).
13. Stolba, *Chem. Zentr.*, 395 (1872).
14. De Boer, J. H. and Van Liempt, J. A. M., "Die Themische Dissoziation der Alkalibofluoroide," *Receuil des Travaux Chimiques des Pays-Bas*, Vol. 46, No. 3, 124-132 (1927).
15. K. S. Pitzer and J. J. Kim, "Thermodynamics of Electrolytes. IV. Activity and Osmotic Coefficients for Mexed Electrolytes," *J. Amer. Chem. Soc.*, 96, 5701-5707 (1974).
16. H. H. Khoo, "Activity Coefficients in Mixed-electrolyte Solutions," *J. Chem. Soc., Faraday Trans. 1*, 82, 1-12 (1986).
17. H-T. Kim and W. J. Frederick, Jr. "Evaluation of Pitzer Ion Interaction Parameters of Aqueous Mixed Electrolyte Solutions at 25°C. 2. Ternary Mixing Parameters," *J. Chem. Eng. Data*, 33, 278-283 (1988).

Appendix A

Hydrofluoric Acid Activity Coefficient

This page is intentionally blank.

Impact of Hydrofluoric Acid Activity Coefficient

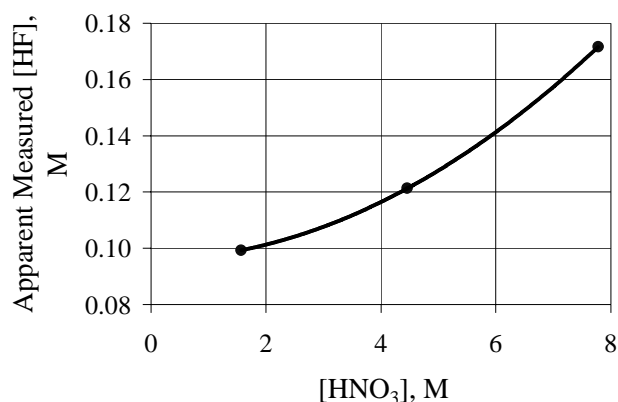
Hydrofluoric acid (HF) is an important reactant in plant process solutions. HF participates in fluoride complexation reactions and metal fluoride precipitating processes. The fluoride complexation of metal ions affects solvent extraction of species such as uranium and plutonium. In the Idaho Nuclear Technology and Engineering Center (INTEC), processes for naval reactor Zircaloy fuels, the HF concentration was typically less than 0.1 molar in less than 1.8 M HNO_3 . Under those conditions, the activity coefficient of HF was near unity. Consequently, the metal fluoride complexation reaction constants could be incorporated into the INEEL chemical equilibrium software that calculated free HF concentration from the speciation of the system without accounting for the effect of HNO_3 on HF activity coefficients.

In the SRS plant solutions, however, the HNO_3 concentrations are significantly higher, up to 6 or 8 molar. Literature data indicate that at HNO_3 concentrations above about 1.8 molar the activity coefficient of 0.1 M HF increases dramatically. Two studies, while showing differing quantitative results, both demonstrate large effects. Vdovenko et al.^{1,2} determined that the activity coefficient (mole fraction basis) of 4 M HF varied from 1.1 to 4.0 as the HNO_3 concentration increased from 0 to 6.6 molar. Breneman and Donohoe³ found that the vapor-phase HF content (over a series of solutions in which the HF concentration was held constant at 0.5 M) increased by a factor of nearly 25 as the HNO_3 concentration was increased from 0 to 14 M. At 0.1 M HF, the increase was not apparent until the HNO_3 concentration exceeded about 1.7 M.

Preliminary experimental work showed that the amperometric response of a metal electrode⁴ selective to HF increases by a factor of 1.7 when the HF concentration is held constant at 0.1 molar and the HNO_3 concentration is increased from 1.6 to 7.8 molar (Figure A-1). Blank experiments with HNO_3 showed no electrode response to HNO_3 . Normally, amperometric measurements respond to concentrations rather than activity. However, the metal electrodes used for the HF measurements create an amperometric current density that is inversely determined by the thickness of an oxide film that is created by reaction of the metal with water and corroded to a steady-state thickness by HF.^{4,5} The HF reaction rate with the oxide film is a function of the HF activity. Therefore, the electrode response is affected by HF activity. At an HF concentration of 0.05 M, the electrode response is unaffected by HNO_3 concentrations up to 1.8 M,⁶ but greater concentrations of either show an effect from HNO_3 .

The observation of the extreme effect of HNO_3 on HF activity is in accord with the expected behavior for hydrogen-bonding solutes.³ As the nitric acid ties up water for solvation, the amount of water available to solvate the hydrofluoric acid drops, thereby increasing the effective HF concentration.⁷ Therefore, for the higher HNO_3 concentrations in the SRS plant solutions, it would be beneficial to determine and incorporate HF activity coefficients as a function of HNO_3 concentration into the INEEL speciation model.

Figure A-1. Effect of HNO₃ Concentration on Ti Electrode
 Measurement of [HF] at 20.9°C
 Standardized [HF] = 0.0927 +/- 0.0001 M



The activity of HF in the solutions is calculated from

$$a_{\text{HF}} = p_{\text{HF}} / K_{\text{HF}}$$

where K_{HF} is the Henry's law constant,¹ 0.46 Torr⁻¹ for HF in water at 25°C and 1 atm total pressure. Then,

$$f_{\text{HF}} = a_{\text{HF}} / m_{\text{HF}}$$

and

$$\gamma_{\text{HF}} = a_{\text{HF}} / N_{\text{HF}}$$

where f_{HF} is the practical activity coefficient and γ_{HF} is the activity coefficient; m_{HF} is molality and N_{HF} is mole fraction of HF in solution.

References for Appendix A

1. V. M. Vdovenko, L. N. Lazarev, and E. V. Shirvinskii, "Study of the Thermodynamic Characteristics of the System HF – HNO₃ – H₂O. I. Measurement of the Vapor Pressure of the Components of the Systems HF – H₂O and HF – HNO₃ – H₂O," *Soviet Radiochemistry*, Vol. 7, No. 1, 45-47 (1965).
2. V. M. Vdovenko, L. N. Lazarev, E. V. Shirvinskii, and Yu. V. Gurikov, "Study of the Thermodynamic Characteristics of the System HF – HNO₃ – H₂O. II. Calculation of the Activity of Components of the System HF – HNO₃ – H₂O," *Soviet Radiochemistry*, Vol. 7 No. 2, 154-160 (1965).
3. K. R. Brenneman and R. J. Donohoe, "Monitoring Hydrofluoric Acid Activity by Vapor-Phase Infrared Spectroscopy," *Appl. Spectroscopy*, Vol. 48, No. 7, 808-812 (1994).

4. J. D. Christian, J. A. Murphy, and D. B. Illum, "Metal Electrodes for Continuous Amperometric Measurement of Free Hydrofluoric Acid in Acidic Solutions Containing Complexing Ions," *Talanta*, **37**, 651-654 (1990).
5. J. A. Murphy, Determination of the Zirconium Fluoride Stability Constants by Direct Measurement of Equilibrium Hydrofluoric Acid Using the Amperometric Response of Titanium and Hafnium Electrodes, WINCO-1098, May 1992; University of Idaho Masters Thesis.
6. J. D. Christian, Idaho Falls, Idaho, unpublished results.
7. I. N. Levine, Physical Chemistry (McGraw-Hill, New York 1978), p. 247.